Disilyl Complexes of Zirconium, Hafnium, and Tantalum. Their Synthesis, Characterization, and Exchanges with Silyl Anions

He Qiu, Hu Cai, Jaime B. Woods, Zhongzhi Wu, Tianniu Chen, Xianghua Yu, and Zi-Ling Xue*

Department of Chemistry, The University of Tennessee, Knoxville, Tennessee 37996

Received April 18, 2005

Cyclopentadienyl-free disilyl amide complexes $[(Me_2N)_3M(SiBu^tPh_2)_2]^-$ (M = Zr, **1**; Hf, **2** as $[Li(THF)_4]^+$ salts), $K(18\text{-crown-}6)_{3/2}\{(Me_2N)_3M[(Me_3Si)_2Si\text{-}(CH_2)_2\text{-}Si(SiMe_3)_2]\}$ (M = Zr, **3**; Hf, **4**), $(Me_2N)_3Ta[Si(SiMe_3)_3]_2$ (**5**), $(Me_2N)_3Ta(SiBu^tPh_2)_2$ (**6**), and $(Me_2N)_3Ta(SiBu^tPh_2)[Si(SiMe_3)_3]$ (**7**) have been prepared. The structures of **1**−**4** have been determined by X-ray single-crystal diffraction. The two $-Si(SiMe_3)_3^-$ ligands in $(Me_2N)_3Ta[Si(SiMe_3)_3]_2$ (**5**) were replaced sequentially by the $-SiBu^tPh_2^-$ anions to give $(Me_2N)_3Ta(SiBu^tPh_2)[Si(SiMe_3)_3]$ (**7**) and $(Me_2N)_3Ta(SiBu^tPh_2)_2$ (**6**). The silyl ligand in $(Me_2N)_3Zr\text{-}Si(SiMe_3)_3$ was found to undergo a reversible exchange with $SiBu^tPh_2^-$, probably through a disilyl intermediate, to reach the following equilibrium: $(Me_2N)_3ZrSi(SiMe_3)_3 + SiBu^tPh_2^- \rightleftharpoons (Me_2N)_3ZrSiBu^tPh_2 + Si(SiMe_3)_3^-$ with $\Delta H° = 4.6(0.5)$ kcal/mol and $\Delta S° = -7(2)$ eu. A similar exchange involving $[(Me_2N)_3M(SiBu^tPh_2)_2]^-$ (M = Zr, **1**; Hf, **2**) was observed: $(Me_2N)_3ZrSiBu^tPh_2 + SiBu^tPh_2^- \rightleftharpoons$ **1** with the estimated free energy of activation $\Delta G^‡ = 14.1(0.5)$ kcal/mol. $(Me_2N)_3Ta(SiBu^tPh_2)_2$ (**6**) and $(Me_2N)_3Ta(SiBu^tPh_2)[Si(SiMe_3)_3]$ (**7**) are thermally unstable. Kinetic studies give the activation parameters of the decomposition of **7**: $\Delta H^‡ = 22.8(1.3)$ kcal/mol and $\Delta S^‡ = -3(5)$ eu.

Silyl derivatives of transition metals are of intense interest for their unique structures, reactivities, and catalytic applications.[1−3] Many early transition metal silyl complexes contain cyclopentadienyl (Cp) ligands or analogous anionic π-ligands,[1] and there are relatively fewer Cp-free d^0 silyl complexes, especially those with two silyl ligands.[2d,4−9] In comparison, multi-alkyl complexes of these transition metals are well known including the peralkyl complexes $M(CH_2R)_n$ ($n = 4$; M = Ti, Zr, Hf; $n = 5$, M = Ta; $n = 6$, M = W).[10] We recently studied Cp-free d^0 transition metal silyl complexes.[11] Novel d^0 bis(silyl) complexes containing two silyl or one chelating disilyl ligand have been prepared: $[(Me_2N)_3M(SiBu^tPh_2)_2]^-$ (M = Zr, **1**;[11] Hf, **2** as $[Li(THF)_4]^+$ salts), $K(18\text{-crown-}6)_{3/2}\{(Me_2N)_3M[(Me_3Si)_2Si\text{-}(CH_2)_2\text{-}Si(SiMe_3)_2]\}$ (M = Zr, **3**; Hf, **4**), $(Me_2N)_3Ta[Si(SiMe_3)_3]_2$ (**5**), $(Me_2N)_3Ta(SiBu^tPh_2)_2$ (**6**), and $(Me_2N)_3Ta(SiBu^tPh_2)[Si(SiMe_3)_3]$ (**7**). The two silyl ligands in $(Me_2N)_3Ta[Si(SiMe_3)_3]_2$ (**5**) were substituted sequentially by the $SiBu^tPh_2^-$ anions to give $(Me_2N)_3Ta(SiBu^tPh_2)[Si(SiMe_3)_3]$ (**7**) and then $(Me_2N)_3Ta(SiBu^tPh_2)_2$ (**6**). In

(1) (a) Tilley, T. D. In *The Silicon-Heteroatom Bond*; Patai, S., Rappoport, Z.; Eds.; Wiley: New York, 1991; Chapters 9 and 10. (b) Eisen, M. S. In *The Chemistry of Organic Silicon Compounds*, Vol. 2; Rappoport, Z.; Apeloig, Y.; Eds.; Wiley: New York, 1998; Part 3, p 2037. (c) Corey, J. Y. In *Advances in Silicon Chemistry*; Larson, G., Ed.; JAI Press: Greenwich, CT, 1991; Vol. 1, p 327. (d) Gauvin, F.; Harrod, J. F.; Woo, H. G. *Adv. Organomet. Chem.* **1998**, *42*, 363. (e) Sharma, H. K.; Pannell, K. H. *Chem. Rev.* **1995**, *95*, 1351. (f) Yu, X.-H.; Morton, L. A.; Xue, Z.-L. *Organometallics* **2004**, *23*, 2210.

(2) (a) Campion, B. K.; Falk, J.; Tilley, T. D. *J. Am. Chem. Soc.* **1987**, *109*, 2049. (b) Arnold, J.; Engeler, M. P.; Elsner, F. H.; Heyn, R. H.; Tilley, T. D. *Organometallics* **1989**, *8*, 2284. (c) Elsner, F. H.; Tilley, T. D.; Rheingold, A. L.; Geib, S. *J. Organomet. Chem*. **1988**, *358*, 169. (d) Heyn, R. H.; Tilley, T. D. *Inorg. Chem*. **1989**, *28*, 1768. (e) Campion, B. K.; Heyn, R. H.; Tilley, T. D. *J. Am. Chem. Soc.* **1990**, *112*, 2011. (f) Radu, N. S.; Engeler, M. P.; Gerlach, C. P.; Tilley, T. D.; Rheingold, A. L. *J. Am. Chem. Soc*. **1995**, *117*, 3621.

(3) (a) Imori, T.; Tilley, T. D. *Polyhedron* **1994**, *13*, 2231. (b) Dioumaev, V. K.; Harrod, J. F. *Organometallics* **1994**, *13*, 1548; **1997**, *16*, 2798. (c) Procopio, L. J.; Carroll, P. J.; Berry, D. H. *Polyhedron* **1995**, *14*, 45. (d) Huhmann, J. L.; Corey, J. Y.; Rath, N. P. *J. Organomet. Chem*. **1997**, *533*, 61. (e) Hengge, E.; Gspaltl, P.; Pinter, E. *J. Organomet. Chem*. **1996**, *521*, 145. (f) Banovetz, J. P.; Suzuki, H.; Waymouth, R. M. *Organometallics* **1993**, *12*, 4700. (g) Verdaguer, X.; Lange, U. E. W.; Reding, M. T.; Buchwald, S. L. *J. Am. Chem. Soc*. **1996**, *118*, 6784. (h) Fu, P.-F.; Marks, T. J. *J. Am. Chem. Soc*. **1995**, *117*, 10747.

(4) (a) Xue, Z.; Li, L.; Hoyt, L. K.; Diminnie, J. B.; Pollitte, J. L. *J. Am. Chem. Soc.* **1994**, *116*, 2169. (b) McAlexander, L. H.; Hung, M.; Li, L.; Diminnie, J. B.; Xue, Z.; Yap, G. P. A.; Rheingold, A. L. *Organometallics* **1996**, *15*, 5231. (c) Diminnie, J. B.; Hall, H. D.; Xue, Z. *Chem. Commun*. **1996**, 2383. (d) Li, L.; Diminnie, J. B.; Liu, X.; Pollitte, J. L.; Xue, Z. *Organometallics* **1996**, *15*, 3520. (e) Diminnie, J. B.; Xue, Z. *J. Am. Chem. Soc.* **1997,** *119*, 12657. (f) Wu, Z.; Diminnie, J. B.; Xue, Z. *Organometallics* **1998**, *17*, 2917. (g) Wu, Z.; McAlexander, L. H.; Diminnie, J. B.; Xue, Z. *Organometallics* **1998**, *17*, 4853. (h) Chen, T.; Wu, Z.; Li, L.; Sorasaenee, K. R.; Diminnie, J. B.; Pan, H.; Guzei, I. A.; Rheingold, A. L.; Xue, Z. *J. Am. Chem. Soc.* **1998**, *120*, 13519. (i) Wu, Z.; Cai, H.; Yu, X.; Blanton, J. R.; Diminnie, J. B.; Pan, H.-J.; Xue, Z. *Organometallics* **2002**, *21*, 3973. (j) Fischer, R.; Zirngast, M.; Folck, M.; Baumgartner, J.; Marschner, C. *J. Am. Chem. Soc.* **2005**, *127*, 70.

(5) Casty, G. L.; Tilley, T. D.; Yap, G. P. A.; Rheingold, A. L. *Organometallics* **1997**, *16*, 4746.

(6) An early reported tetrasilyl complex $Ti(SiPh_3)_4$ was found later to be $Ti(OSiPh_3)_4$. (a) Hengge, E.; Zimmermann, H. *Angew. Chem., Int. Ed. Engl*. **1968**, *7*, 142. (b) Kingston, B. M.; Lappert, M. F. *J. Chem. Soc., Dalton Trans*. **1972**, 69.

(7) $Ti(SiMe_3)_4$ was reported to exist at −78 °C, but no characterization was offered for this complex. Razuvaev, G. A.; Latyaeva, V. N.; Vyshinskaya, L. I.; Malysheva, A. V.; Vasileva, G. A. *Dokl. Akad. Nauk. SSSR* **1977**, *237*, 605.

(8) Several zerovalent Zr-polytin complexes have been reported. (a) $[K(15\text{-crown-}5)_2]_2[Zr(CO)_5(SnMe_3)_2]$: Ellis, J. E.; Yuen, P.; Jang, M. *J. Organomet. Chem*. **1996**, *507*, 283. (b) $[n\text{-}Pr_4N]_2[(Ph_3Sn)_4M(CO)_4]$ (M = Zr, Hf): Ellis, J. E.; Chi, K. M.; DiMaio, A. J.; Frerichs, S. R.; Stenzel, J. R.; Rheingold, A. L.; Haggerty, B. S. *Angew. Chem., Int. Ed. Engl.* **1991**, *30*, 194.

10.1021/om050302f CCC: $30.25
Publication on Web 07/16/2005

addition, the silyl ligand in $(Me_2N)_3Zr\text{-}Si(SiMe_3)_3$ undergoes an exchange with $SiBu^tPh_2^-$, probably through a disilyl intermediate. The preparation of these new disilyl complexes, structures of **1**−**4**, and studies of the silyl exchanges and thermal decomposition of **6** and **7** are reported here.

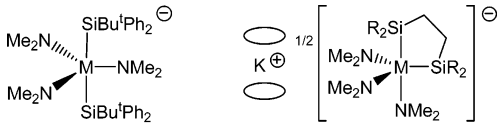

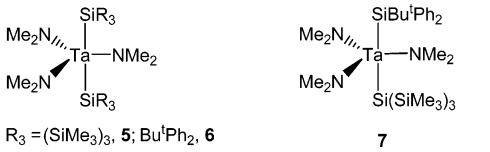

Experimental Section

All manipulations were performed under a dry nitrogen atmosphere with the use of either a drybox or standard Schlenk techniques. Solvents were purified by distillation from potassium/benzophenone ketyl and stored under nitrogen prior to use. $TaCl_5$ (Strem) was sublimed prior to use. $(Me_2N)_3MCl$ (M = Zr; Hf),[12a] $(Me_2N)_3MSiBu^tPh_2(THF)_{0.5}$ (M = Zr; Hf),[12b] $(Me_2N)_3TaCl_2$,[13] $(Me_2N)_3Ta(SiBu^tPh_2)Cl$,[4i] $[K(18\text{-crown-6})]_2[(Me_3Si)_2Si(CH_2)_2Si(SiMe_3)_2]$ (**8**),[14] $Li(THF)_3Si(SiMe_3)_3$,[15a] and $Li(THF)_3SiBu^tPh_2$[15b] were prepared according to the literature procedures. Benzene-d_6, THF-d_8, and toluene-d_8 were dried over activated molecular sieves. ^1H and $^{13}C\{^1H\}$ NMR spectra were recorded on a Bruker AC-250 or AMX-400 spectrometer and referenced to solvent (residual protons in the ^1H spectra). $^{29}Si\{^1H\}$ data were obtained by a Bruker AMX-400 spectrometer and referenced to $SiMe_4$. Elemental analyses were performed by Complete Analysis Laboratories Inc., Parsippany, NJ.

For the thermodynamic studies, the equilibrium constants K_{eq} were obtained from ^1H NMR spectra. At least two separate experiments were conducted at a given temperature. The *maximum* random uncertainty in the equilibrium constants was combined with the estimated systematic uncertainty, ca. 5%. The estimated uncertainty in the temperature measurements for an NMR probe was 1 K. The enthalpy ($\Delta H°$) and entropy ($\Delta S°$) changes were calculated from an unweighted nonlinear least-squares procedure contained in the SigmaPlot Scientific Graph System. The uncertainties in $\Delta H°$ and $\Delta S°$ were computed from the following error propagation formulas, which were derived from $-RT \ln K_{eq} = \Delta H° - T\Delta S°$:[16]

$$(\sigma\Delta H°)^2 = (\sigma T/T)^2R^2(T_{max}{}^2T_{min}{}^4 + T_{min}{}^2T_{max}{}^4)[\ln(K_{eq(max)}/K_{eq(min)})]^2/\Delta T^4 + 2R^2T_{max}{}^2T_{min}{}^2(\sigma K_{eq}/K_{eq})^2/\Delta T^2$$

$$(\sigma\Delta S°)^2 = 2R^2T_{min}{}^2T_{max}{}^2[\ln(K_{eq(max)}/K_{eq(min)})]^2(\sigma T/T)^2/\Delta T^4 + R^2(T_{max}{}^2 + T_{min}{}^2)(\sigma K_{eq}/K_{eq})^2/\Delta T^2$$

where $\Delta T = (T_{max} - T_{min})$; $\sigma T = 1$ K; T = the mean of T_{min} and T_{max}.[17]

Preparation of $[Li(THF)_4][(Me_2N)_3Zr(SiBu^tPh_2)_2]$ (1 as a $[Li(THF)_4]^+$ salt). To a solution of $(Me_2N)_3ZrSiBu^tPh_2(THF)_{0.5}$ (0.568 g, 1.14 mmol) in 3 mL of toluene was added 1 equiv of $Li(THF)_3SiBu^tPh_2$ (0.534 g, 1.14 mmol) in 3 mL of toluene at room temperature. **1** gradually crystallizes from the solution as orange crystals (0.75 g, 0.75 mmol, 66% yield). ^1H NMR (benzene-d_6, 250.1 MHz, 23 °C): δ 7.87, 7.34, 7.20 (m, 20H, C_6H_5), 3.41 (m, 16H, OCH_2CH_2), 2.82 (s, 18H, NMe_2), 1.40 (b, 18H, $SiCMe_3$), 1.29 (m, 16H, OCH_2CH_2). $^{13}C\{^1H\}$ NMR (benzene-d_6, 62.9 MHz, 23 °C): δ 149.1, 137.2, 127.1, 125.8 (C_6H_5), 68.2 (OCH_2CH_2), 40.6 (NMe_2), 31.3 ($SiCMe_3$), 25.4 (OCH_2CH_2), 21.3 ($SiCMe_3$). Anal. Calcd for $C_{54}H_{88}N_3O_4Si_2LiZr$: C, 65.01; H, 8.89. Found: C, 65.18; H, 8.78.

Preparation of $[Hf(NMe_2)_3(SiBu^tPh_2)_2][Li(THF)_4]$ (2 as a $[Li(THF)_4]^+$ salt). $Hf(NMe_2)_3(SiBu^tPh_2)(THF)_{0.5}$ (0.293 g, 0.500 mmol) was mixed with $Li(THF)_3SiBu^tPh_2$ (0.231 g, 0.499 mmol). To this mixture, 3 mL of toluene was added at room temperature. Yellow crystals of **2** precipitated immediately (0.368 g, 0.339 mmol, 68% yield). ^1H NMR (benzene-d_6, 400.11 MHz, 23 °C): δ 8.04−7.17 (m, 20H, C_6H_5), 3.42 (m, 16H, OCH_2CH_2), 2.83 (s, 18H, NMe_2), 1.53 and 1.29 (two broad peaks, $SiCMe_3$), 1.29 (m, 16H, OCH_2CH_2). $^{13}C\{^1H\}$ NMR (benzene-d_6, 100.62 MHz, 23 °C): δ 137.35, 137.11, 136.06, 127.50, 127.26, 126.86, 124.76 (C_6H_5), 68.11 (OCH_2CH_2), 39.33 (NMe_2), 31.89 and 30.26 (two broad peaks, $SiCMe_3$), 27.64 ($SiCMe_3$), 25.42 (OCH_2CH_2). A NOESY spectrum revealed an exchange of the two $[SiBu^tPh_2]^-$ groups in **2**. Anal. Calcd for $C_{54}H_{88}N_3O_4Si_2HfLi$: C, 59.78; H, 8.18. Found: C, 59.64; H, 7.95.

Preparation of $K(18\text{-crown-6})_{3/2}\{(Me_2N)_3Zr[(Me_3Si)_2Si(CH_2)_2Si(SiMe_3)_2]\}$ (3). $(Me_2N)_3ZrCl$ (0.203 g, 0.687 mmol) and $[K(18\text{-crown-6})]_2[(Me_3Si)_2Si(CH_2)_2Si(SiMe_3)_2]$ (**8**, 0.675 g, 0.686 mmol) were added to a Schlenk flask and then dissolved in toluene (5 mL). After 45 min of stirring, all volatiles were removed in vacuo. The resulting mixture of a yellow-orange solid and oil was washed with hexanes to give bright yellow powders of **3**. The yellow powders were dissolved in toluene. An oil formed at the bottom of the flask. The flask containing the oil and the toluene solution was kept in a freezer at −30 °C for two weeks to give crystals of **3**·toluene (0.592 g, 83.3% yield). In a separate experiment, the yellow powders were dissolved in benzene, and the solution was filtered. Removal in vacuo of volatiles in the filtrate, followed by washing of the

(9) For metallocene-based disilyl complexes of early transition and lanthanide metals, see, e.g., $Cp_2Zr(SiMe_3)[Si(SiMe_3)_3]$;[2a] $Cp_2Ti(SiPh_3)_2$;[6b] $Cp_2Ti(SiPh_2)_5$: Igonin, V. A.; Ovchinnikov, Yu. E.; Dementev, V. V.; Shklover, V. E.; Timofeeva, T. V.; Frunze, T. M.; Struchkov, Yu. T. *J. Organomet. Chem.* **1989**, *371*, 187. $Cp_2Ti(SiPh_2)_4$: Holtman, M. S.; Schram, E. P. *J. Organomet. Chem.* **1980**, *187*, 147. $Cp_2Ta(H)(SiMe_2H)_2$: Jiang, Q.; Carroll, P. J.; Berry, D. H. *Organometallics* **1991**, *10*, 3648. $[Cp_2Ln(SiMe_3)_2][Li(DME)_2]$ (Ln = Sm, Lu): Schumann, H.; Nickel, S.; Hahn, E.; Heeg, M. J. *Organometallics* **1985**, *4*, 800. $Cp_2M[Si(SiMe_3)_3]_2$ (M = Zr, Hf): Kayser, C.; Frank, D.; Baumgartner, J.; Marschner, C. *J. Organomet. Chem.* **2003**, *667*, 149. $Cp_2NbH(SiCl_3)_2$: Dorogov, K. Yu.; Churakov, A. V.; Kuzmina, L. G.; Howard, J. A. K.; Nikonov, G. I. *Eur. J. Inorg. Chem.* **2004**, 771, and references therein.

(10) (a) Li, L.; Hung, M.; Xue, Z. *J. Am. Chem. Soc.* **1995**, *117*, 12746. (b) Davidson, P. J.; Lappert, M. F.; Pearce, R. *Chem. Rev.* **1976**, *76*, 219. (c) Schrock, R. R.; Parshall, G. W. *Chem. Rev.* **1976**, *76*, 243. (d) Wu, Y.-D.; Chan, K. W. K.; Xue, Z. *J. Am. Chem. Soc.* **1995**, *117*, 9259. (e) Wu, Y.-D.; Peng, Z.-H.; Xue, Z. *J. Am. Chem. Soc.* **1996**, *118*, 9772.

(11) Wu, Z.; Diminnie, J. B.; Xue, Z. *J. Am. Chem. Soc*. **1999**, *121*, 4300.

(12) (a) Wu, Z.; Diminnie, J. B.; Xue, Z. *Inorg. Chem*. **1998**, *37*, 2570. (b)Wu, Z.; Diminnie, J. B.; Xue, Z. *Inorg. Chem*. **1998**, *43*, 6366.

(13) Chisholm, M. H.; Huffman, J. C.; Tan, L.-S. *Inorg. Chem*. **1981**, *20*, 1859.

(14) Blanton, J. R.; Diminnie, J. B.; Chen, T.; Wiltz, A. M.; Xue, Z. *Organometallics* **2001**, *20*, 5542. For related potassium silyl complexes, see, e.g.: (a) Marschner, C. *Eur. J. Inorg. Chem.* **1998**, 221. (b) Jenkins, D. M.; Teng, W.; Englich, U.; Stone, D.; Ruhlandt-Senge, K. *Organometallics* **2001**, *20*, 4600. (c) Teng, W.; Ruhlandt-Senge, K. *Organometallics* **2004**, *23*, 2694. (d) Fischer, R.; Konopa, T.; Ully, S.; Baumgartner, J.; Marschner, C. *J. Organomet. Chem*. **2003**, *685*, 79.

(15) (a) Gutekunst, G.; Brook, A. G. *J. Organomet. Chem*. **1982**, *225*, 1. (b) Campion, B. K.; Heyn, R. H.; Tilley, T. D. *Organometallics* **1993**, *12*, 2584.

(16) Levine, I. N. *Physical Chemistry*, 3rd ed.; McGraw-Hill: New York, 1988; pp. 307−309.

(17) Taylor, J. R. *An Introduction to Error Analysis. The Study of Uncertainties in Physical Measurements*; University Science Books: Mill Valley, CA, 1982; Chapter 4, p 93.

solid with hexanes, yielded an analytically pure solid of **3**. ^{1}H NMR (250.1 MHz, benzene-d_6, 23 °C): δ 3.56 (s, 18H, NMe_2), 3.32 (s, 36H, O−CH_2), 1.63 (s, 4H, Si−CH_2), 0.67 (s, 36H, SiMe_3). ^{1}H NMR (250.1 MHz, toluene-d_8, 23 °C): δ 3.50 (s, 18H, NMe_2), 3.35 (s, 36H, O−CH_2), 1.56 (s, 4H, Si−CH_2), 0.59 (s, 36H, SiMe_3). ^{1}H NMR (400.1 MHz, THF-d_8, 23 °C): δ 3.63 (s, 36H, O−CH_2), 2.99 (s, 18H, NMe_2), 1.07 (s, 4H, Si−CH_2), 0.51 (s, 36H, SiMe_3). ^{13}C{^{1}H} NMR (62.9 MHz, benzene-d_6, 23 °C): δ 70.30 (O−CH$_2$), 44.64 (NMe_2), 15.83 (Si−CH$_2$), 4.52 (SiMe_3). ^{13}C{^{1}H} NMR (62.9 MHz, toluene-d_8, 23 °C): δ 70.71 (O−CH$_2$), 44.60 (NMe_2), 15.82 (Si−CH$_2$), 4.43 (SiMe_3). ^{13}C{^{1}H} NMR (100.6 MHz, THF-d_8, 23 °C): δ 71.20 (O−CH$_2$), 44.50 (NMe_2), 15.61 (Si−CH$_2$), 4.12 (SiMe_3). ^{29}Si{^{1}H} NMR (79.5 MHz, THF-d_8, 23 °C): δ −8.01 (SiMe$_3$), −73.11 (Si−SiMe$_3$). Anal. Calcd for the toluene-free solid of **3**, $C_{38}H_{94}KN_3O_9Si_6Zr$: C, 44.06; H, 9.15. Found: C, 43.89; H, 9.08.

Preparation of K(18-crown-6)$_{3/2}${(Me$_2$N)$_3$Hf[(Me$_3$Si)$_2$Si(CH$_2$)$_2$Si(SiMe$_3$)$_2$]} (4). To a mixture of (Me$_2$N)$_3$HfCl (0.300 g, 0.867 mmol) and [K(18-crown-6)]$_2$[(Me$_3$Si)$_2$Si(CH$_2$)$_2$Si(SiMe$_3$)$_2$] (**8**, 0.863 g, 0.878 mmol) was added toluene (15 mL). All volatiles were removed in vacuo after the reaction mixture was stirred for 45 min. The resulting brown solid was washed with hexanes (3 × 15 mL) to give a bright yellow solid. This solid was dissolved in toluene, and the oil-containing solution was cooled at −35 °C to give yellow crystals of **4**·toluene (0.494 g, 0.439 mmol, 51% yield). ^{1}H NMR (400.0 MHz, THF-d_8, 23 °C): δ 3.61 (s, 36H, O−CH_2), 3.01 (s, 18H, NMe_2), 1.19 (s, 4H, Si−CH_2), 0.59 (s, 36H, SiMe_3). ^{13}C{^{1}H} NMR (100.60 MHz, THF-d_8, 23 °C): δ 71.37 (O−CH$_2$), 44.31 (NMe_2), 15.73 (Si−CH$_2$), 4.23 (SiMe_3). ^{29}Si{^{1}H} NMR (79.5 MHz, THF-d_8, 23 °C): δ −5.5 (SiMe$_3$), −48.8 (SiSiMe$_3$). The crystals of **4**·toluene were washed with pentane, and the solid was then dried in vacuo. ^{1}H NMR of the solid showed that there was one toluene molecule per three molecules of **4** in the solid. This sample was then submitted for elemental analysis. Anal. Calcd for $C_{121}H_{290}K_3N_9O_{27}Si_{18}Hf_3$: C, 41.98; H, 8.44. Found: C, 41.67; H, 8.32.

Preparation of (Me$_2$N)$_3$Ta[Si(SiMe$_3$)$_3$]$_2$ (5). To a yellow slurry of (Me$_2$N)$_3$TaCl$_2$ (0.511 g, 1.33 mmol) in pentane (25 mL) was added 2 equiv of Li(THF)$_3$Si(SiMe$_3$)$_3$ (1.25 g, 2.66 mmol) at room temperature. The reaction solution immediately turned deep purple. After stirring for 3 h at room temperature, the volatiles were removed in vacuo, yielding a purple solid. Extraction of the solid with pentane, followed by filtration and crystallization at −20 °C, afforded deep red crystals of **5** (0.31 g, 0.38 mmol, 29% yield). ^{1}H NMR (toluene-d_8, 400.1 MHz, −30 °C): δ 3.22 (s, 18H, NMe_2), 0.37 (s, 54H, SiMe_3). ^{13}C{^{1}H} NMR (toluene-d_8, 100.6 MHz, −30 °C): δ 44.9 (NMe_2), 6.5 (SiMe_3). ^{29}Si{^{1}H} NMR (DEPT, toluene-d_8, 79.5 MHz, −30 °C): δ 0.95 (SiSiMe$_3$), −6.25 (SiSiMe$_3$). Anal. Calcd for $C_{24}H_{72}N_3Si_8Ta$: C, 35.65; H, 8.98. Found: C, 35.42; H, 8.75.

Preparation of (Me$_2$N)$_3$Ta(SiBu^{t}Ph$_2$)$_2$ (6). Li(THF)$_2$SiBu^{t}Ph$_2$ (0.041 g, 0.11 mmol) was added to a mixture of (Me$_2$N)$_3$TaCl$_2$ (0.020 g, 0.052 mmol) and 4,4′-dimethylbiphenyl (0.010 g, 0.055 mmol) in benzene-d_6 at room temperature. After 10 min, **6** was observed by NMR (0.041 mmol, 78% yield). **6** was found thermally unstable, and it decomposed to HSiBu^{t}Ph$_2$ and other unknown species. The structural assignment for **6** was thus based on its spectroscopic data. ^{1}H NMR (benzene-d_6, 250.1 MHz): δ 7.58−7.14 (m, 20H, C$_6H_5$), 2.99 (s, 18H, NMe_2), 1.07 (s, 18H, CMe_3). ^{13}C{^{1}H} NMR (benzene-d_6, 62.9 MHz): δ 148.7, 137.3, 127.1, 126.8 (C_6H$_5$), 44.5 (NMe_2), 31.1 (CMe_3), 24.2 (CMe$_3$). ^{29}Si{^{1}H} NMR (benzene-d_6, 79.5 MHz): δ 48.9 (Si-Bu^{t}Ph$_2$).

Preparation of (Me$_2$N)$_3$Ta(SiBu^{t}Ph$_2$)[Si(SiMe$_3$)$_3$] (7). (Me$_2$N)$_3$Ta(SiBu^{t}Ph$_2$)Cl (0.022 g, 0.037 mmol) in benzene-d_6 was treated with Li(THF)$_3$Si(SiMe$_3$)$_3$ (0.017 g, 0.036 mmol) and 4,4′-dimethylbiphenyl (0.014 g, 0.077 mmol) at room temperature. The reaction solution immediately turned purple. **7** was observed by NMR (0.031 mmol, 86% yield). The complex was found unstable at room temperature, and it decomposed to HSiBu^{t}Ph$_2$, HSi(SiMe$_3$)$_3$, and other unknown species. The structural assignment for **7** was thus based on its spectroscopic data. ^{1}H NMR (benzene-d_6, 250.1 MHz): δ 7.61−7.15 (m, 10H, C$_6H_5$), 3.14 (s, 18H, NMe_2), 1.08 (s, 9H, CMe_3), 0.32 (s, 27H, SiMe_3). ^{13}C{^{1}H} NMR (benzene-d_6, 62.9 MHz): δ 147.3, 137.2, 127.2, 127.1 (C_6H$_5$), 44.8 (NMe_2), 30.9 (CMe_3), 24.7 (CMe$_3$), 6.8 (SiMe_3). ^{29}Si{^{1}H} NMR (benzene-d_6, 79.5 MHz, 8 °C): δ 40.9 (SiBu^{t}Ph$_2$), −11.1 (SiSiMe$_3$), −19.8 (SiSiMe$_3$).

Kinetic Study of the Decomposition of (Me$_2$N)$_3$Ta(SiBu^{t}Ph$_2$)$_2$ (6) and (Me$_2$N)$_3$Ta(SiBu^{t}Ph$_2$)[Si(SiMe$_3$)$_3$] (7). Complex **7** was prepared in situ at 23 °C from a 1:1 mixture of (Me$_2$N)$_3$Ta(SiBu^{t}Ph$_2$)Cl and Li(THF)$_3$Si(SiMe$_3$)$_3$ in a toluene-d_8 solution containing 4,4′-dimethylbiphenyl as an internal standard. The NMR spectrometer was preset to the temperature between 298 and 323 K, and ^{1}H spectra were recorded. Complex **6** was also prepared in situ from a mixture of 1 equiv of (Me$_2$N)$_3$TaCl$_2$ and 2 equiv of Li(THF)$_3$SiBu^{t}Ph$_2$ in a toluene-d_8 solution containing 4,4′-dimethylbiphenyl as an internal standard. At least two separate experiments were conducted at a given temperature. The *maximum* random uncertainty in the rate constants was combined with the estimated systematic uncertainty, ca. 5%. The estimated uncertainty in the temperature measurements for an NMR probe was 1 K. The activation enthalpy ($\Delta H^{\ddagger}$) and entropy ($\Delta S^{\ddagger}$) were calculated from the Eyring equation using an unweighted nonlinear least-squares procedure contained in the SigmaPlot Scientific Graph System. The uncertainties in $\Delta H^{\ddagger}$ and $\Delta S^{\ddagger}$ were computed from the error propagation formulas derived by Girolami and co-workers.[18]

The kinetics of the decomposition of **6** was conducted at 303 K.

X-ray Crystal Structure Determination of 1, 2, 3·toluene, and 4·toluene. The crystal structure of **1** was determined on a Siemens R3m/V diffratometer equipped with a Nicolet LT-2 low-temperature device. A suitable crystal was coated with Paratone oil and mounted under a stream of nitrogen at −100 °C. The unit cell parameters and orientation matrix were determined from a least-squares fit of the orientation of at least 25 reflections obtained from a rotation photograph and an automatic peak search routine. Intensity data were measured with graphite-monochromated Mo Kα radiation (λ = 0.71073 Å). Background counts were measured at the beginning and the end of each scan with the crystal and counter kept stationary. The intensities of three standard reflections were measured after every 97 reflections. The intensity data were corrected for Lorentz and polarization effects and an empirical absorption correction based upon ψ scans. The structure was solved by direct methods using the Siemens SHELXTL 93 (version 5.0) proprietary software package. All hydrogen atoms were placed in calculated positions and introduced into the refinement as fixed contributors with an isotropic U value of 0.008 Å^2.

The crystal structures of **2**, **3**·toluene, and **4**·toluene were determined on a Bruker AXS Smart 1000 X-ray diffratometer with Mo Kα radiation. Yellow crystals were selected in Paratone oil and mounted on a hairloop under a N_2 stream at −100 °C. The structures of **2**, **3**·toluene, and **4**·toluene were solved by direct methods. Non-hydrogen atoms in **2** were anistropically refined. In SHELXTL, the normal L.S. 4 procedure was performed to refine non-hydrogen atoms isotropically. The L.S. 4 procedure could not be used in the anisotropic refinement because of the large size of the cell. The CGLS procedure is much faster and more suitable in most macromolecule refinements.[20,21] Hence the CGLS and, subsequently, the L.S./BLOC procedures were used in the next, anisotropic refinement. The CGLS procedure does not provide estimated standard deviations (esd), therefore, in the final refinement,

(18) Morse, P. M.; Spencer, M. D.; Wilson, S. R.; Girolami, G. S. *Organometallics* **1994**, *13*, 1646.

(19) See Supporting Information for details.

Scheme 1

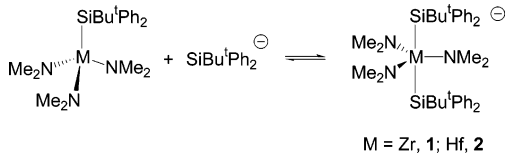

M = Zr, **1**; Hf, **2**

Scheme 2

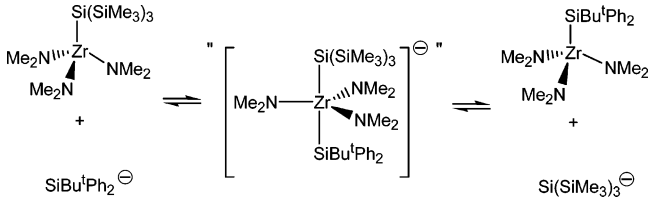

L.S. 1 and BLOC 1 procedures were used to obtain estimated standard deviations of bond lengths and bond angles in **3**·toluene and **4**·toluene. All hydrogen atoms were included in the structure factor calculation at idealized positions and were allowed to ride on the neighboring atoms with relative isotropic displacement coefficients. The SHELXTL (version 5.1) proprietary software package was used for all structure solution and refinement calculations.

Results and Discussion

Preparation and Characterization of Disilyl Complexes 1−7. The anionic disilyl complexes [M(NMe$_2$)$_3$(SiBu^{t}Ph$_2$)$_2$][Li(THF)$_4$] (M = Zr, **1**; Hf, **2** as [Li(THF)$_4$]$^+$ salts) were prepared by the addition of Li(THF)$_3$SiBu^{t}Ph$_2$[15b] to (Me$_2$N)$_3$M(SiBu^{t}Ph$_2$)[12b] in toluene, from which [Li(THF)$_4$]·**1** and [Li(THF)$_4$]·**2** crystallized at room temperature (Scheme 1). [Li(THF)$_4$]·**1** is thermally unstable in solution but may be stored indefinitely as a solid at −20 °C.

There is a sharp −NMe$_2$ signal in the ^{1}H and ^{13}C{^{1}H} NMR spectra of **1** or **2** at room temperature. Both ^{1}H (400.1 MHz) and ^{13}C{^{1}H} (100.6 MHz) NMR peaks of the Bu^t groups in the Zr complex **1** are *broad* at 23 °C, and at 0 °C, these resonances of the Bu^t groups resolve into two separate broad signals, which are close to those of (Me$_2$N)$_3$Zr(SiBu^{t}Ph$_2$)[12b] and Li(THF)$_3$SiBu^{t}Ph$_2$. This indicates that the −SiBu^{t}Ph$_2$ ligand in (Me$_2$N)$_3$Zr(SiBu^{t}Ph$_2$)[12b] is in a rapid exchange with Li(THF)$_3$SiBu^{t}Ph$_2$ in solution at room temperature (Scheme 1). The dynamic NMR of this exchange reaction in **1** was studied in the current work. The signals of the two −SiBu^{t}Ph$_2$ ligands were found to coalesce at 20 °C. The free energy of activation $\Delta G^{\ddagger}$ was estimated to be 14.1(0.5) kcal/mol for the exchange in **1** at the coalescence temperature. A similar exchange was also observed in the Hf analogue **2**. Unlike the exchange in its Zr analogue **1**, both ^{1}H (400.1 MHz) and ^{13}C{^{1}H} (100.6 MHz) NMR spectra of **2** at 23 °C show two broad peaks for the Bu^t groups. The coalescence of the peaks does not occur until 43 °C. The free energy of activation $\Delta G^{\ddagger}$ was estimated to be 15.3(0.5) kcal/mol for the exchange in **2** at the coalescence temperature. This is slightly higher than 14.1(0.5) kcal/mol for the exchange in the Zr analogue **1**. 2-D HMQC spectra of **1** and **2** were used to confirm NMR assignments. In addition, the exchange in **2** was observed in its 2-D NOESY spectrum.

The silyl ligand in (Me$_2$N)$_3$Zr-Si(SiMe$_3$)$_3$ was found to undergo a reversible exchange with the SiBu^{t}Ph$_2^-$ anion as well to reach the following equilibrium: (Me$_2$N)$_3$ZrSi(SiMe$_3$)$_3$ + SiBu^{t}Ph$_2^-$ ⇌ (Me$_2$N)$_3$Zr-SiBu^{t}Ph$_2$ + Si(SiMe$_3$)$_3^-$. Although this exchange does not involve disilyl complexes, it was studied in the current work to provide a better understanding of silyl exchanges in d^0 transition metal complexes. Once Li(THF)$_3$SiBu^{t}Ph$_2$ was added to the solution of (Me$_2$N)$_3$Zr-Si(SiMe$_3$)$_3$, (Me$_2$N)$_3$Zr-SiBu^{t}Ph$_2$ and Li(THF)$_3$Si(SiMe$_3$)$_3$ were observed in the solution at room temperature (Scheme 2). The equilibrium constants for the exchange were measured between 263 and 293 K from ^{1}H NMR spectra and are listed in Table 1. A plot of ln K_{eq} vs 1/T (Figure 1) gave a linear fit and yielded ΔH° = 4.6(0.5) kcal/mol and ΔS° = −7(2) eu.[16]

The reaction of (Me$_2$N)$_3$MCl[12a] (M = Zr, Hf) with [K(18-crown-6)]$_2$[(Me$_3$Si)$_2$Si-(CH$_2$)$_2$-Si(SiMe$_3$)$_2$] (**8**) in toluene was found to give chelating disilyl complexes **3** and **4** (Scheme 3).

The concentrations of both (Me$_2$N)$_3$MCl[12a] and [K(18-crown-6)]$_2$[(Me$_3$Si)$_2$Si(CH$_2$)$_2$Si(SiMe$_3$)$_2$] (**8**)[14] were found to be important to the success of the preparation. Solids

Table 1. Equilibrium Constants (K_{eq}) for (Me$_2$N)$_3$Zr-Si(SiMe$_3$)$_3$ + SiBu^{t}Ph$_2^-$ ⇌ (Me$_2$N)$_3$Zr-SiBu^{t}Ph$_2$ + Si(SiMe$_3$)$_3^-$

T (K)	$[K_{eq} \pm \delta K_{eq(ran)}]$[a]
293(1)	82.83(0.02)
288(1)	89.82(0.01)
283(1)	101.73(0.03)
278(1)	125.42(0.02)
273(1)	145.95(0.01)
268(1)	173.03(0.03)
263(1)	192.51(0.01)

[a] The total uncertainty $\sigma K_{eq}/K_{eq}$ of 6% was calculated from $\sigma K_{eq(ran)}/K_{eq}$ = 3%, and the estimated systematic uncertainty $\sigma K_{eq(sys)}/K_{eq}$ = 5% by $\sigma K_{eq}/K_{eq} = [(\sigma K_{eq(ran)}/K_{eq})^2 + (\sigma K_{eq(sys)}/K_{eq})^2]^{1/2}$.

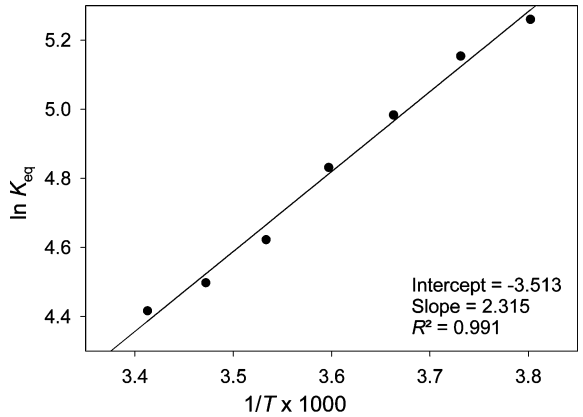

Figure 1. Plot of ln K_{eq} vs 1/T of the equilibrium (Me$_2$N)$_3$Zr-Si(SiMe$_3$)$_3$ + SiBu^{t}Ph$_2^-$ ⇌ (Me$_2$N)$_3$Zr-SiBu^{t}Ph$_2$ + Si(SiMe$_3$)$_3^-$.

Scheme 3

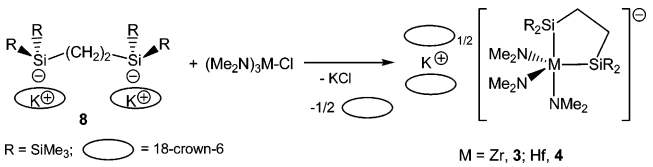

R = SiMe$_3$; ⬭ = 18-crown-6

M = Zr, **3**; Hf, **4**

(20) Sheldrick, G. M. *A Program for Empirical Absorption Correction of Area Detector Data*; University of Gottingen: Gottingen, Germany, 1996.

(21) Sheldrick, G. M. *A Program for the Refinement of Crystal Structures*; University of Gottingen: Gottingen, Germany, 1997.

Scheme 4

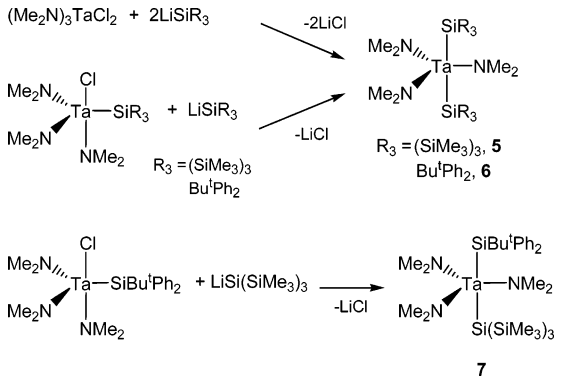

Table 2. ^{29}Si NMR of Complexes Containing the $-SiPh_2Bu^t$ or $-Si(SiMe_3)_3$ Ligands

$[Li(THF)_3]SiBu^tPh_2$[a,15b]	7.54 (*Si*Bu^{t}Ph$_2$)
$[Li(THF)_3]Si(SiMe_3)_3$[a,15a]	−185.4 [*Si*(SiMe$_3$)$_3$]
	−5.3 (Me$_3$*Si*)
$(Me_2N)_3$Zr-SiBu^{t}Ph$_2$·0.5 THF[b,12b]	19.6 (*Si*Bu^{t}Ph$_2$)
$(Me_2N)_3$Zr-Si(SiMe$_3$)$_3$[b,12b]	−4.4 (*Si*Me$_3$)
	−124.6 [*Si*(SiMe$_3$)$_3$]
$(Me_2N)_3$Hf-SiBu^{t}Ph$_2$·0.5 THF[b,12b]	46.8 (*Si*Bu^{t}Ph$_2$)
$(Me_2N)_3$Hf-Si(SiMe$_3$)$_3$[b,12b]	−2.1 (*Si*Me$_3$)
	−103.5 [*Si*(SiMe$_3$)$_3$]
Cp$_2$Hf(SiBu^{t}Ph$_2$)Me[b,22]	49.04 (*Si*Bu^{t}Ph$_2$)
Cp$_2$Hf[Si(SiMe$_3$)$_3$]Me[b,22]	−84.12 [*Si*(SiMe$_3$)$_3$]
$(Me_2N)_3$Ta(SiBu^{t}Ph$_2$)Cl[b,4i]	64.6 (*Si*Bu^{t}Ph$_2$)
$(Me_2N)_3$Ta[Si(SiMe$_3$)$_3$]Cl[b,4i]	4.39 (*Si*Me$_3$)
	−51.34 [*Si*(SiMe$_3$)$_3$]
$(Me_2N)_4$Ta-SiBu^{t}Ph$_2$ [b,4i]	−189.0 (*Si*Bu^{t}Ph$_2$)
$(Me_2N)_4$Ta-Si(SiMe$_3$)$_3$ [b,4i]	−4.0 (*Si*Me$_3$)
	−98.4 [*Si*(SiMe$_3$)$_3$]
$(Me_2N)_3$Ta(SiBu^{t}Ph$_2$)$_2$ (**6**)[b]	48.94 (*Si*Bu^{t}Ph$_2$)
$(Me_2N)_3$Ta[Si(SiMe$_3$)$_3$]$_2$ (**5**)[b]	0.95 (*Si*Me$_3$)
	−6.25 [*Si*(SiMe$_3$)$_3$]
$(Me_2N)_3$Ta(SiBu^{t}Ph$_2$)[Si(SiMe$_3$)$_3$] (**7**)[c]	40.9 (*Si*Bu^{t}Ph$_2$)
	−11.1 (Si*Si*Me$_3$)
	−19.8 (*Si*SiMe$_3$)

[a] Benzene-d_6. [b] Room temperature, benzene-d_6. [c] 8 °C, benzene-d_6.

of both reagents were mixed in one flask and dissolved in a small amount of toluene (5−15 mL) to start the reaction. The products, after washing with hexanes, were crystallized from toluene at −30 °C to give crystals of **3**·toluene or **4**·toluene.

Four resonances were observed in the ^{1}H NMR spectra of **3** and **4**, respectively. In the ^{1}H NMR spectrum of **3**, the −Si*Me*$_3$ resonance (0.67 ppm) of the disilyl ligand and −O−C*H*$_2$ resonances (3.32 ppm) of 18-crown-6, respectively, are only slightly shifted from those in [K(18-crown-6)]$_2$[(Me$_3$Si)$_2$Si-(CH$_2$)$_2$-Si(SiMe$_3$)$_2$] (**8**). The −C*H*$_2$− resonance in **3** is 0.3 ppm downfield shifted from that of **8**. Only one resonance attributed to the −NMe$_2$ ligands was observed at 23 °C in the ^{1}H NMR spectrum of **3** at 250 MHz. However, in the ^{1}H NMR spectrum of **3** at 400 MHz, two nearly overlapping amide and −SiMe$_3$ peaks were found at 23 °C, which were more separated at lower temperatures,[19] suggesting dynamic exchanges of these groups. In the ^{13}C{^{1}H} NMR spectra of **3** in benzene-d_6, the −SiMe$_3$ resonance of **3** at 4.48 ppm is upfield shifted from that (5.74 ppm) in [K(18-crown-6)]$_2$[(Me$_3$Si)$_2$Si(CH$_2$)$_2$Si(SiMe$_3$)$_2$] (**8**). One −NMe$_2$ peak was observed for **3** at 44.61 ppm at 23 °C. In the ^{29}Si{^{1}H} NMR spectrum of **3** at 23 °C, the Zr−*Si*−SiMe$_3$ peak at −73.11 ppm is consistent with those in other Zr−Si complexes such as (Me$_3$CCH$_2$)$_3$Zr-*Si*(SiMe$_3$)$_3$ (−85.5 ppm), (Me$_3$SiCH$_2$)$_3$Zr-*Si*(SiMe$_3$)$_3$ (−75.7 ppm),[4a,b] and Cp$_2$Zr[*Si*(SiMe$_3$)$_3$]Cl (−85.5 ppm).[2a] In the ^{29}Si NMR spectra of its Hf analogue **4**, the Hf−*Si*−SiMe$_3$ peak was observed at −48.8 ppm. In comparison, the α-Si resonances of, for example, (Me$_2$N)$_3$Hf-*Si*-Bu^{t}Ph$_2$·0.5THF, CpCp*Hf(*Si*Bu^{t}Ph$_2$)Cl,[22] and (Me$_2$N)$_3$-Hf-*Si*(SiMe$_3$)$_3$[12b] were observed at 46.8, 51.48, and −103.5 ppm, respectively.

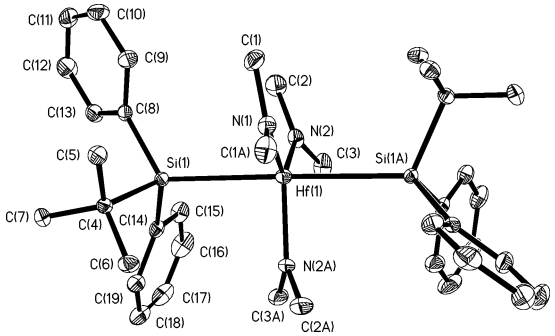

Figure 2. ORTEP diagram of the bis(silyl) anion in **2**, showing 35% thermal ellipsoids.

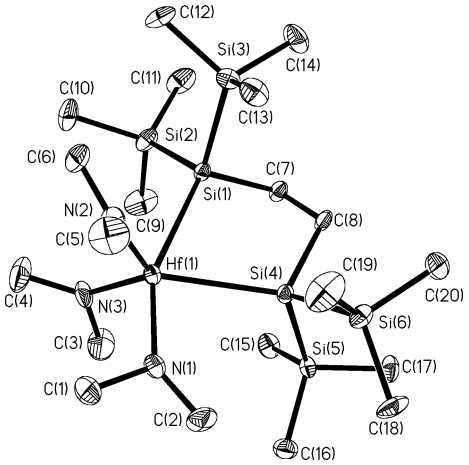

Figure 3. ORTEP diagram of the anion in bis(silyl) Hf complex **4**·toluene, showing 30% thermal ellipsoids.

No exchange between the chelating silyl ligands in **4** and excess Li(THF)$_3$SiBu^{t}Ph$_2$ was observed after the two species were mixed in THF-d_8 for 24 h. This is perhaps not surprising, as the substitution of the chelating [(Me$_3$Si)$_2$Si(CH$_2$)$_2$Si(SiMe$_3$)$_2$]$^{2-}$ ligand in **4** by the mono silyl SiBu^{t}Ph$_2^-$ anion is thermodynamically unfavorable.

The tantalum disilyl complex (Me$_2$N)$_3$Ta[Si(SiMe$_3$)$_3$]$_2$ (**5**) was readily prepared either by the reactions of the silyl chloride complex (Me$_2$N)$_3$Ta[Si(SiMe$_3$)$_3$]Cl with 1 equiv of Li(THF)$_3$Si(SiMe$_3$)$_3$ or by the reaction of (Me$_2$N)$_3$-TaCl$_2$ with 2 equiv of Li(THF)$_3$Si(SiMe$_3$)$_3$ (Scheme 3). (Me$_2$N)$_3$Ta(SiBu^{t}Ph$_2$)$_2$ (**6**), an analogue of **5**, was similarly prepared. The mixed bis(silyl) complex (Me$_2$N)$_3$-Ta(SiBu^{t}Ph$_2$)[Si(SiMe$_3$)$_3$] (**7**) was prepared from the reaction of (Me$_2$N)$_3$Ta(SiBu^{t}Ph$_2$)Cl[4i] with 1 equiv of Li(THF)$_3$Si(SiMe$_3$)$_3$ (Scheme 4).

The NMR spectra of **5**−**7** are consistent with the structural assignment of the complexes. The ^{1}H NMR spectra of bis(silyl) complexes **5**−**7** show only one resonance for −NMe$_2$ ligands at both low and room temperatures, suggesting that **5**−**7** may adopt a trigonal

(22) Sadow, A. D.; Tilley, T. D. *J. Am. Chem. Soc.* **2003**, *125*, 9462.

Table 3. Crystal Data of 1, 2, 3·toluene, and 4·toluene

		1 ($C_{54}H_{88}Li\ N_3O_4Si_2Zr$)	**2** ($C_{54}H_{88}LiN_3O_4Si_2Hf$)	**3**·toluene ($C_{180}H_{408}K_4N_{12}O_{36}Si_{24}Zr_4$)	**4**·toluene ($C_{180}H_{408}K_4N_{12}O_{36}Si_{24}Hf_4$)
fw		997.61	1084.88	4512.60	4861.68
cryst syst		monoclinic	monoclinic	triclinic	triclinic
space group		*C*2/*c*	*C*2/*c*	$P\bar{1}$	$P\bar{1}$
lattice params	*a* (Å)	21.195(6)	21.139(4)	13.077(3)	13.114(7)
	b (Å)	17.434(5)	17.466(3)	24.797(5)	24.704(14)
	c (Å)	17.801(5)	17.762(3)	41.823(8)	41.71(2)
	α (deg)	90	90	101.06(3)	100.870(9)
	β (deg)	119.76(2)	119.699(3)	92.00(3)	91.881(9)
	γ (deg)	90	90	101.05(3)	101.425(10)
V (Å^3)		5710(3)	5696.8(17)	13028(5)	12974(12)
Z		4	4	2	2
d_{calcd} (Mg m^{-3})		1.160	1.265	1.153	1.248
μ (mm^{-1})		0.277	1.916	0.388	1.828
F(000)		2144	2272	4888	5144
θ (deg)		1.61−22.54	1.61−28.30	1.07−27.05	1.00−28.99
no. of data collected		3880	29 219	119 093	141 993
completeness			96.8% to $\theta = 28.30°$	92.4% to $\theta = 27.05°$	89.2% to $\theta = 28.99°$
no. of indep data		3761 ($R_{int} = 0.0256$)	6865 ($R_{int} = 0.0642$)	52 829 ($R_{int} = 0.1100$)	61 492 ($R_{int} = 0.0670$)
no. of data/restraints/ params		3758/0/295	13 215/2/599	52 829/0/2419	61 492/0/2420
index ranges		$0 \le h \le 22$	$-23 \le h \le 23$	$-16 \le h \le 16$	$-17 \le h \le 17$
		$0 \le k \le 18$	$-23 \le k \le 23$	$-30 \le k \le 30$	$-33 \le k \le 33$
		$-19 \le l \le 16$	$-25 \le l \le 25$	$-52 \le l \le 52$	$-55 \le l \le 55$
R indices [$I > 2\sigma(I)$]		R1 = 0.0465	R1 = 0.0401	R1 = 0.1076	R1 = 0.0621
		wR2 = 0.1240	wR2 = 0.1096	wR2 = 0.2790	wR2 = 0.1476
goodness-of-fit on F^2		1.083	0.907	0.991	0.965

[a] $wR2 = [\sum w(F_o^2 - F_c^2)^2/\sum w(F_o^2)^2]^{1/2}$; $R = \sum||F_o| - |F_c||/\sum|F_o|$; $w = 1/[\sigma^2(F_o^2) + (aP)^2 + bP]$; $P = [2F_c^2 + \mathrm{Max}(F_o^2,0)]/3$.

bipyramidal structure with two silyl ligands in the axial and three amide ligands in the equatorial positions. In the ^{29}Si NMR spectra of $(Me_2N)_3Ta[Si(SiMe_3)_3]_2$ (**5**) and $(Me_2N)_3Ta(SiBu^tPh_2)_2$ (**6**), the α-Si resonances appear at −6.25 (*Si*$SiMe_3$) and 48.9 (*Si*Bu^tPh_2) ppm, respectively. This follows the general trend of chemical shifts for the silyl ligands $-Si(SiMe_3)_3$ and $-SiBu^tPh_2$ in the complexes listed in Table 2: The former usually is further upfield shifted than the latter with the exception of $(Me_2N)_4Ta$-$SiBu^tPh_2$ and $(Me_2N)_4Ta$-$Si(SiMe_3)_3$. On the basis of this observation, the two α-Si resonances in $(Me_2N)_3Ta(SiBu^tPh_2)[Si(SiMe_3)_3]$ (**7**) at 40.9 and −19.8 ppm are assigned to those of $-Si$$Bu^tPh_2$ and $-Si$$SiMe_3$, respectively. Thermal decomposition of **7**, to be discussed below, prevented us from taking more scans during the NMR data acquisition to observe the $^1J_{Si-Si}$ couplings, which would have helped the assignment.

When a solution of $(Me_2N)_3Ta[Si(SiMe_3)_3]_2$ (**5**) in benzene-d_6 was added to $Li(THF)_3SiBu^tPh_2$, the formation of $(Me_2N)_3Ta(SiBu^tPh_2)[Si(SiMe_3)_3]$ (**7**), $(Me_2N)_3Ta(SiBu^tPh_2)_2$ (**6**), and $Li(THF)_3Si(SiMe_3)_3$ was observed, indicating that one $-Si(SiMe_3)_3^-$ ligand in **5** was substituted by a $-SiBu^tPh_2^-$ anion to give **7**. Subsequently, the remaining $-Si(SiMe_3)_3^-$ ligand in **7** was replaced by another $-SiBu^tPh_2^-$ anion to give **6**. **6** was found, however, to be inert to the exchange with the $-Si(SiMe_3)_3^-$ anion. Both **6** and **7** are thermally unstable and decompose to silanes and unknown species. The kinetic studies of their decompositions are discussed below.

Crystal and Molecular Structures of 1, 2, 3·toluene, and 4·toluene. ORTEP views of the bis(sily) anion **1** and **4**·toluene are shown in Figures 2 and 3. ORTEP views of **1** and **3** with structures similar to those of **2** and **4**, respectively, are given in the Supporting Information.[19] The crystallographic data of **1**, **2**, **3**, and **4** are summarized in Table 3. Selected bond distances and bond angles of **2** and **4** are given in Table 4.

Table 4. Selected Bond Distances (Å) and Bond Angles (deg) in 2 and 4[19]

$[(Me_2N)_3Hf(SiBu^tPh_2)_2]^-$ in **2**			
Hf(1)−N(2)	2.035(16)	Hf(1)−N(1)	2.029(15)
Hf(1)−N(3)	2.063(5)	Hf(1)−Si(1)	2.918(7)
Hf(1)−Si(2)	2.896(7)		
N(2)−Hf(1)−N(1)	117.9(2)	N(2)−Hf(1)−N(3)	119.7(8)
N(1)−Hf(1)−N(3)	122.5(9)	N(2)−Hf(1)−Si(1)	93.5(4)
N(1)−Hf(1)−Si(1)	89.8(4)	N(3)−Hf(1)−Si(1)	88.6(6)
N(2)−Hf(1)−Si(2)	86.4(4)	N(1)−Hf(1)−Si(2)	88.2(4)
N(3)−Hf(1)−Si(2)	93.4(6)	Si(1)−Hf(1)−Si(2)	177.71(15)

$(Me_2N)_3Hf[(Me_3Si)_2Si(CH_2)_2Si(SiMe_3)_2]^-$ in **4**			
Hf(1)−N(3)	2.043(7)	Hf(1)−N(2)	2.047(7)
Hf(1)−N(1)	2.063(7)	Hf(1)−Si(1)	2.846(2)
Hf(1)−Si(4)	2.863(2)	C(7)−C(8)	1.554(10)
C(7)−Si(1)	1.945(7)	C(8)−Si(4)	1.960(8)
N(3)−Hf(1)−N(2)	109.4(3)	N(3)−Hf(1)−N(1)	97.2(3)
N(2)−Hf(1)−N(1)	97.9(3)	N(3)−Hf(1)−Si(1)	96.8(2)
N(2)−Hf(1)−Si(1)	96.1(2)	N(1)−Hf(1)−Si(1)	155.7(2)
N(3)−Hf(1)−Si(4)	126.3(2)	N(2)−Hf(1)−Si(4)	123.5(2)
N(1)−Hf(1)−Si(4)	84.9(2)	Si(1)−Hf(1)−Si(4)	70.78(7)
C(8)−C(7)−Si(1)	108.4(5)	C(7)−C(8)−Si(4)	111.1(5)

In the structure of **2** (Figure 2), the Hf atom is five-coordinate to form an anion with two silyl ligands and three $-NMe_2$ ligands. The two $-SiBu^tPh_2$ ligands, which are trans to each other, occupy the axial positions to form trigonal bipyramidal geometry in **2** with the nearly linear Si−Hf−Si angle of 177.93(5)°. Unlike the trigonal bipyramidal anion $[(Me_2N)_3Hf(SiBu^tPh_2)_2]^-$ (**2**), the $\{(Me_2N)_3Hf[(Me_3Si)_2Si$-$(CH_2)_2$-$Si(SiMe_3)_2]\}^-$ anion in **4** (Figure 3) is severely distorted from either the trigonal bipyramidal or the square pyramidal geometry. In this case the two Si atoms in the chelating bisilyl ligand are cis to each other in the pseudoaxial and pseudoequatorial positions, respectively, with the Si−Hf−Si angle of 70.8°. The Hf−Si bond lengths [2.846(2)−2.863(2) Å] in **4** are slightly shorter than [2.896(7)−2.918(7) Å] in

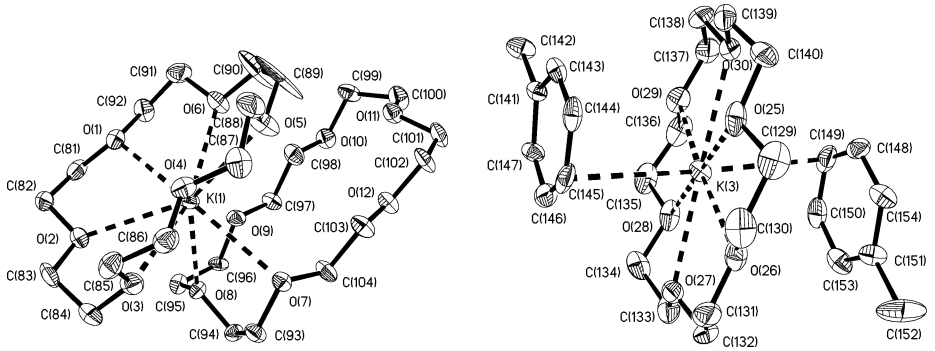

Figure 4. ORTEP diagram of the cations in two different molecules of **4**·toluene, showing 30% thermal ellipsoids.[19]

Scheme 5

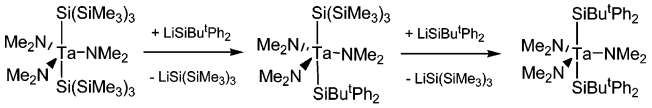

$[(Me_2N)_3Hf(SiBu^tPh_2)_2]^-$ (**2**). In comparison, the Hf–Si bond [2.807(4) Å] in the monosilyl complex $(Me_2N)_3Hf$-$SiPh_2{}^tBu$ is shorter than in both **2** and **4**.[12b] The Hf–N bond lengths [2.043(7)–2.063(7) Å] are also similar to 2.029(3)–2.063(5) Å in $(Me_2N)_3Hf(SiBu^tPh_2)_2$ (**2**) and 2.019(9)–2.030(9) Å in $(Me_2N)_3HfSiBu^tPh_2$.[12b]

There are two types of cations in **4** (Figure 4): K(18-crown-6)$^+$ and K(18-crown-6)$_2{}^+$. The K^+ ion in the former was coordinated to one 18-crown-6 ligand. There is also weak interaction between K^+ and two toluene molecules. In the latter, the two 18-crown-6 ligands use six and two O atoms, respectively, to bond to the K^+ ion.

The triamide disilyl complexes **5**–**7** may adopt a trigonal bipyramidal structure with the two silyl ligands in the axial positions (Scheme 5), as observed in the triamide disilyl anion **1**. However, we were not able to obtain a crystal structure of these disilyl Ta compounds. **6** and **7** were thermally unstable, which is discussed below. Crystals of **5** were found to rapidly decompose on the X-ray diffractometer, precluding attempts to confirm its structure.

Kinetic Studies of the Decomposition of $(Me_2N)_3Ta(SiBu^tPh_2)_2$ (6) and $(Me_2N)_3Ta(SiBu^tPh_2)[Si(SiMe_3)_3]$ (7). Both **6** and **7** are thermally unstable and decompose at 23 °C to $HSiBu^tPh_2$, $HSiBu^tPh_2$, and $HSi(SiMe_3)_3$, respectively, and other unknown species. **5**, containing two $-Si(SiMe_3)_3$ ligands, is thermally stable at room temperature under nitrogen.

The decomposition reactions were not characterized, and not all products of the thermal decomposition are known. To compare the rates of the decomposition of the two complexes, the decomposition kinetics was studied. The decomposition was found to follow first-order (irreversible) kinetics. The sample of **7** used in the kinetic studies was prepared in situ from **5** and 1 equiv of $Li(THF)_3Si(SiMe_3)_3$ in toluene-d_8. The kinetic studies were conducted between 298 and 323 K in toluene-d_8 to give plots of $\ln(C_0/C)$ (C = [**7**]) vs time t (Figure 5) and the first-order rate constants k of the conversion (Table 5). An Eyring plot (Figure 6) gives activation parameters of the thermal decomposition: $\Delta H^{\ddagger} = 22.8(1.3)$ kcal/mol, $\Delta S^{\ddagger} = -3(5)$ eu, and $\Delta G^{\ddagger}_{298\ K} = 24(3)$ kcal/mol.

Table 5. Rate Constants k for the Decomposition of 7[a]

T (K)	$[k \pm \delta k_{(ran)}] \times 10^5$ (s^{-1})
298(1)	2.48(0.01)
303(1)	4.33(0.16)
308(1)	8.7(0.3)
313(1)	16.9(0.3)
318(1)	31.9(1.7)
323(1)	47.1(0.7)

[a] The total uncertainty of $\delta k/k = 7.3\%$ was calculated from $\delta k_{(ran)}/k = 5.3\%$ and $\delta k_{(sys)}/k = 5\%$.

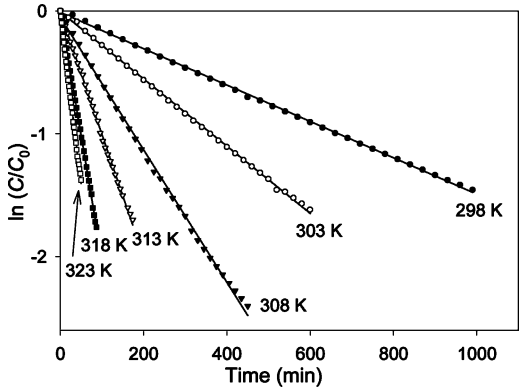

Figure 5. Kinetic plots of the thermal decomposition of **7**.

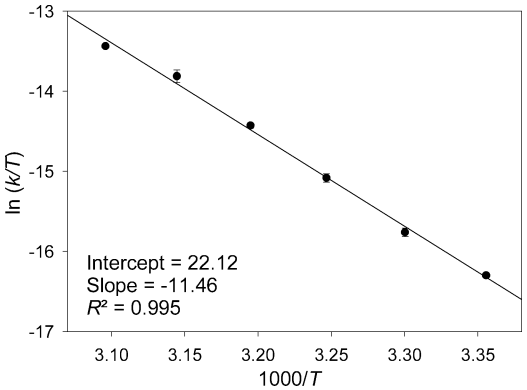

Figure 6. Eyring plot of the thermal decomposition of **7**.

The thermal decomposition of **6** was studied by NMR in toluene-d_8. The decomposition was found to follow the first-order kinetics as well. The rate constant k for this decomposition at 303 K is $7.2(0.2) \times 10^{-5}$ s^{-1}, larger than the rate constant [$4.33(0.16) \times 10^{-5}$ s^{-1}, Table 5] for the thermal decomposition of **7** at this temperature, suggesting that **7**, with one $-Si(SiMe_3)_3$ and one $-Si-$

Bu^tPh_2 ligand, decomposes slower than **6**, containing two $-SiBu^tPh_2$ ligands.

Acknowledgment is made to the National Science Foundation (CHE-9457368, CHE-9904338, and CHE-0212137), DuPont Young Professor Award, and the Camille Dreyfus Teacher-Scholar program for financial support of the research. We thank the reviewers for helpful suggestions.

Supporting Information Available: This material is available free of charge via the Internet at http://pubs.acs.org.

OM050302F